Available online at www.sciencedirect.com
SCIENCE DIRECT®
ELSEVIER
Nuclear Instruments and Methods in Physics Research B 207 (2003) 28–35
NIM B Beam Interactions with Materials & Atoms
www.elsevier.com/locate/nimb

# Size effects in the irradiation-induced crystalline-to-amorphous transformation

Al Meldrum [a,*], Lynn A. Boatner [b], Rodney C. Ewing [c]

[a] *Department of Physics, University of Alberta, Edmonton, Canada AB T6G 2J1*
[b] *Oak Ridge National Laboratory, Oak Ridge, TN 37831, USA*
[c] *Department of Nuclear Engineering and Radiological Sciences, Ann Arbor, MI 48109, USA*

**Abstract**

Due to their unique properties, nanocrystalline composites are currently finding applications in high-radiation environments. By using zirconia ($ZrO_2$) as an example, we show that at the smallest particle sizes, radiation damage effects can be strongly enhanced, and that under certain conditions, materials that are generally considered to be radiation resistant can become susceptible to irradiation-induced amorphization. Bulk zirconia has previously been irradiated to 680 dpa with no evidence of amorphization; however, we find that nanocrystalline zirconia can be amorphized at a dose as low as 0.9 dpa due, in part, to the energetics of the increased surface-to-volume ratio. These results have implications for the design of nanocomposite materials for use in space vehicles and in other high-radiation environments.
© 2003 Elsevier Science B.V. All rights reserved.

*PACS:* 64.70.N; 61.82.R; 61.46; 61.82.R
*Keywords:* Nanocrystals; Amorphization; $ZrO_2$; Irradiation; Zirconia

## 1. Introduction

The general phenomenon of radiation effects in solids is a mature field, having been developed over the past five decades. In fact, the earliest investigations of radiation damage in materials date back to the 19th century, when mineral scientists first studied the unusual structural properties of uranium- and thorium-bearing minerals [1]. However, it was not until the 1950s that the need for radiation-resistant materials became more pressing and systematic research programs on radiation–solid interactions were initiated. Understanding the behavior of materials under various types of irradiation has important implications in the areas of the disposal of nuclear waste, geochronology and in the development of materials for use in nuclear reactors. The radiation-induced behavior of hundreds of different materials has been investigated, and the basic physical processes that cause radiation damage are reasonably well understood. Generalized theoretical models that predict a given material's response to irradiation have been developed and are relatively successful (e.g. see [2] and references therein).

* Corresponding author. Tel.: +1-780-492-5342; fax: +1-780-492-0714.
*E-mail address:* ameldrum@ualberta.ca (A. Meldrum).

0168-583X/03/$ - see front matter © 2003 Elsevier Science B.V. All rights reserved.
doi:10.1016/S0168-583X(03)00519-6

Despite the considerable body of literature now existing on the effects of irradiation on bulk materials, there have been essentially no systematic studies of the behavior of *nanocrystalline* materials under similar conditions. Nanocomposite materials have a range of applications in various radiation environments, and they may become an integral component of space exploration vehicles – either as lightweight, high-strength materials for structural components, or as electronic sensors and switches. In the case of microelectronics applications, radiation damage effects such as single event upsets can potentially become more pronounced in nanodevices [3].

Recent investigations have shown that the thermodynamics of phase transitions in nanocrystalline materials can be considerably altered as compared with that characteristic of the corresponding bulk phase. As an example, high-pressure solid–solid phase transitions may have a large hysteresis because of the lack of nucleation sites in crystallographically "perfect" nanoparticles (e.g. [4]). Melting points can be either raised or lowered by hundreds of degrees due to surface energy effects. The irradiation-induced crystalline-to-amorphous (c–a) transition represents another important type of solid transformation, however, despite the long history of radiation damage studies, the effects of particle size on the c–a transition have never been systematically investigated. We are aware of only one report, in which Si nanocrystals embedded in a matrix of fused $SiO_2$ were reported to become amorphous under irradiation conditions for which bulk silicon does not normally amorphize [5].

Recent work has clearly demonstrated that the effects of particle sizes on solid phase transitions can be large – therefore, for the present study, we chose to investigate the effects of ion irradiation on an assemblage of $ZrO_2$ nanoparticles. $ZrO_2$ is employed in superplastic structural ceramics that demonstrate excellent strength and fracture toughness, and it is also used as an oxygen sensor and a fast ion conductor [6]. Most importantly for this study, it is recognized as one of the most radiation-resistant ceramics known to exist. Bulk $ZrO_2$ has previously been irradiated with a wide spectrum of energetic particles, and it does not show any significant susceptibility to amorphization, even at cryogenic temperatures and doses up to 680 displacements per atom (dpa) (e.g. [7,8]). If, in the present experiment, $ZrO_2$ nanoparticles were amorphized by ion irradiation, the results would indicate that small-particle size effects play a major role in the energetics of the radiation induced c–a transition. The work presented as part of these conference proceedings is an extension of a recently published investigation in which we first documented the unusual behavior of $ZrO_2$ nanoparticles under irradiation [9].

At room temperature, zirconia is monoclinic and the Zr cations are coordinated with seven oxygen atoms. At ~1200 °C [10], a martensitic-type phase transition occurs. The higher temperature phase is a tetragonal derivative of the fluorite structure, with each Zr coordinated to eight oxygen atoms. At ~2400 °C [10], tetragonal $ZrO_2$ undergoes another structural phase transition to form a true cubic fluorite structure that is stable up to the melting temperature of ~2700 °C. The cubic and tetragonal phases cannot be quenched, but they can be stabilized at room temperature by the replacement of Zr with up to 15 mol.% of larger cations, such as the lanthanides or yttrium. The addition of these trivalent oxides requires vacancies in the oxygen sublattice, and therefore, cubic stabilized zirconia has fewer than two oxygen atoms per formula unit.

## 2. Experimental

All of the experiments were performed in situ in a transmission electron microscope (TEM) at the IVEM Facility at Argonne National Laboratory. We first formed a $ZrO_2$ nanocrystal composite in a TEM specimen by the decomposition of ion-beam amorphized $ZrSiO_4$ (e.g. [11]). This produces an assemblage of randomly oriented $ZrO_2$ nanocrystals embedded in a matrix of amorphous $SiO_2$ (Fig. 1). Next, the $ZrO_2$ nanocrystal composite was irradiated with 1.0 MeV $Xe^{2+}$ ions (flux = $6.25 \times 10^{11}$ ions/cm$^2$/s), and the microstructural evolution was followed by bright- and dark-field imaging and electron diffraction. At this energy, over 99% of the Xe ions pass through the thin

TEM foil. The irradiation fluence was converted to units of dose in displacements per atom using SRIM-2000 [12] in order to calculate the number of displacements-per-ion per-unit-depth, using a displacement energy of 40 eV for both Zr and O.

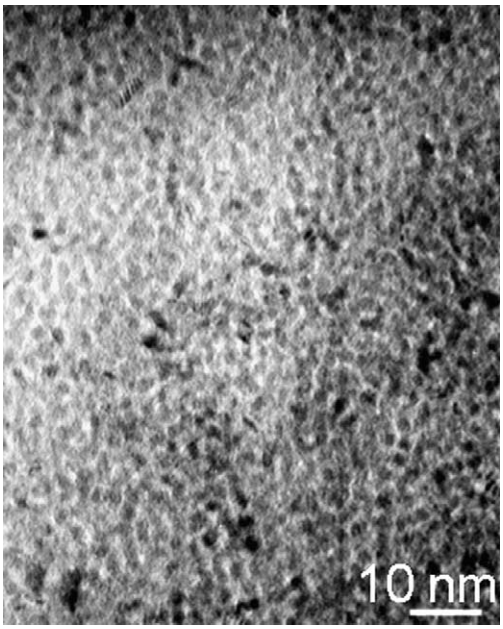


Fig. 1. Bright field image of an assemblage of $ZrO_2$ nanoclusters after thermal precipitation from ion-beam-amorphized $ZrSiO_4$. The particles average 3 nm in diameter and are dispersed randomly throughout an $SiO_2$ matrix.

## 3. Results

After the thermal decomposition step, the specimen consisted of randomly oriented $ZrO_2$ nanocrystals embedded throughout a matrix of amorphous $SiO_2$. In this respect, the specimens were qualitatively similar to the ion implanted silicon nanocrystals whose enhanced susceptibility to radiation-induced amorphization was recently reported [5]. Measurements of ~200 $ZrO_2$ particles in high-resolution TEM images gave an average radius of ~1.5 nm. Electron diffraction measurements using digital intensity scans showed that the nanoparticles were, in fact, tetragonal zirconia (Fig. 2). The diffraction patterns were indexed to card #17-0923 in the JCPDS database. Another structure of tetragonal $ZrO_2$ also exists (card #42-1164) that provides an equally good index match. In previous work, we were unaware of this and indexed to alternate structures [9,13]. Dark-field images using the bright (1 1 1) diffraction ring have a "patchy" appearance, indicating some degree of local texturing in the $ZrO_2$ nanocomposite (Fig. 3(a)).

When the 1.0 MeV $Xe^{2+}$ ion beam was turned on, the bright regions corresponding to the $ZrO_2$

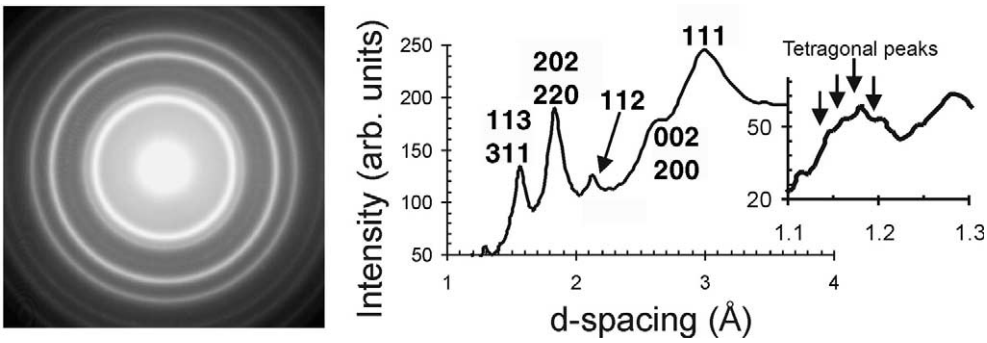


Fig. 2. Electron diffraction pattern and corresponding digital intensity scan from the specimen in Fig. 1. The diffraction pattern is indexed to card #17-0923 in the JCPDS database. Cubic zirconia has no lattice spacing that corresponds to the (1 1 2) diffraction maximum marked by the arrow in the figure. The inset shows an enlargement of the region between 1.1 and 1.3 Å. Scattering intensities from cubic zirconia are especially weak in this region; whereas the observed peaks are relatively strong, further supporting the identification of tetragonal $ZrO_2$.

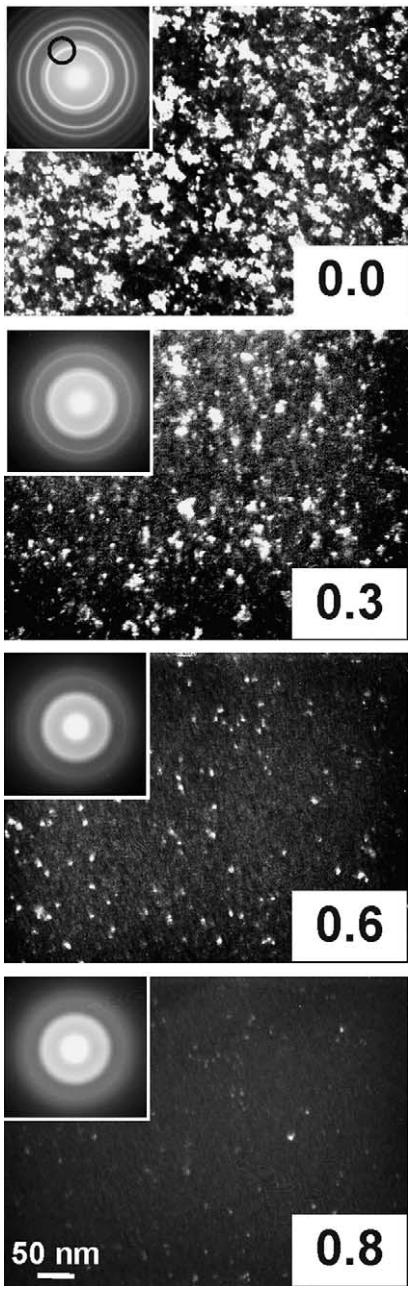


Fig. 3. Sequence of dark field images taken with the objective aperture centered around the bright $(1\,0\,1)_{tetragonal}$ ring, as shown in the topmost diffraction pattern. Crystalline $ZrO_2$ nanoparticles appear as bright patches in the image. The ion dose is given in the bottom right corner of each panel.

nanocrystals in the dark-field images became progressively fainter (Fig. 3(b)–(d)). The (1 1 2) diffraction ring also disappeared, indicating that a structural transformation from tetragonal to cubic zirconia occurred as the irradiation proceeded. Continuing the irradiation further weakened the remaining diffraction rings, and the bright "patches" in the dark-field images continued to disappear. Finally, at a dose of 0.9 dpa, the sample was uniform in contrast, and the diffraction pattern showed only a diffuse halo characteristic of an amorphous material. During these observations we found that the electron beam inhibited the amorphization process, so we minimized exposure of the specimen during the TEM observations.

The experiment was repeated over a range of temperatures up to 450 °C. The dose for amorphization increased exponentially with temperature (Fig. 4), until at 475 °C, it was no longer possible to amorphize the $ZrO_2$ nanocomposite. Several of the temperature-dependent measurements were repeated to ensure reproducibility. Although the same general trends were observed (increasing dose with increasing temperature), there was significant variability in the results (up to 50% at the higher temperatures). We attribute this to the effects of electron beam irradiation during our observations and to variations in the sample thickness, which also had a significant effect on the measured amorphization dose.

Since there are currently no analytical capabilities on the IVEM instrument, the chemical

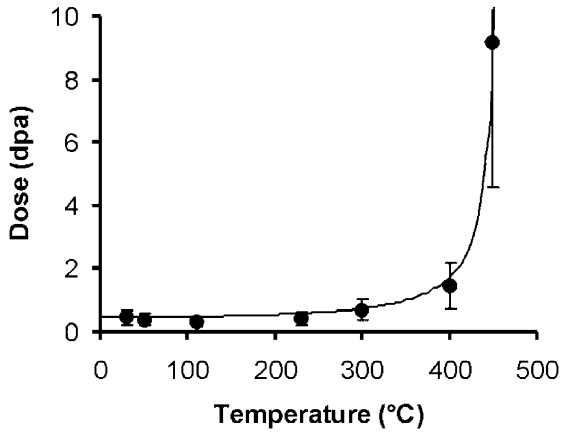


Fig. 4. Temperature dependence of the amorphization dose for the $ZrO_2$ nanocluster composite. The line was fit with a model consistent with defect-driven amorphization [14].

composition of the nanocrystal-containing specimens prior to and after irradiation was determined using energy-dispersive X-ray analysis (EDX) in a JEOL 2010 TEM at the University of Alberta. Using the original $ZrSiO_4$ as a standard for determining the $k$-factors, the composition of the nanocomposite prior to and after amorphization can be obtained with reasonable accuracy using standard peak fitting and background subtraction procedures. Both specimens were slightly enriched in Zr relative to Si, especially along the thin edges of the sample. The ion-beam-amorphized nanocomposite had some areas containing as much as 85% $ZrO_2$ by weight. Due to the small size of the nanoparticles with respect to the specimen thickness, this does not represent the composition of individual nanoparticles but does show that some regions of the amorphized specimen are considerably depleted in Si.

## 4. Discussion

In previous experiments, bulk $ZrO_2$ has been irradiated to doses as high as 680 dpa, with no evidence for amorphization [15]. Nevertheless, structural transformations do occur in irradiated zirconia. For example, it is commonly reported that monoclinic $ZrO_2$ transforms to either the tetragonal or cubic structure during irradiation, but once this occurs, there are no further transitions. This stabilization of the tetragonal structure probably occurs as a result of accumulated oxygen vacancies [16], producing a net stoichiometry similar to that of chemically stabilized cubic zirconia. There is, however, one report of the formation of a buried amorphous layer after high dose implantation of Cs into cubic-stabilized zirconia [17]. In that experiment, the chemistry was considerably modified by the presence of 10 at.% of an implanted element (Cs) that is incompatible with the $ZrO_2$ structure. The fact that so much Cs was required to induce amorphization further supports the extreme radiation resistance of this material.

In the present study, the starting material consisted of tetragonal $ZrO_2$ nanocrystals embedded with random orientations in amorphous $SiO_2$. However, monoclinic $ZrO_2$ is the stable polymorph at room temperature. The stabilization of tetragonal zirconia can be explained by a simple thermodynamic analysis. Although monoclinic $ZrO_2$ has a lower free energy at room temperature, its surface energy ($\gamma$) is actually higher than that of the tetragonal phase (for an incoherent interface, as is the case here, $\gamma = 1.10$ and 1.46 J/m$^2$ for tetragonal and monoclinic zirconia, respectively) [18]. Therefore, there should exist a critical size at which the total free energy of the two phases is equal. A simple equation to calculate this critical radius was derived over two decades ago in a classic paper [18]:

$$r_c = \frac{-3\Delta\gamma}{\Delta\psi + \Delta\varepsilon}. \quad (1)$$

Here, $\Delta\gamma$ is the surface energy difference between the tetragonal and monoclinic phases (0.36 J/m$^2$), $\Delta\psi$ is the free energy difference for an infinite crystal, and $\Delta\varepsilon$ is the change in internal strain energy for embedded particles. $\Delta\psi$ is equal to $q(1 - T/T_b)$ where $q$ is the heat of transformation per unit volume ($-2.82 \times 10^8$ J/m$^3$ ) and $T_b$ is bulk transformation temperature ($\sim$1450 K). The strain energy term for our system is not known; however, for tetragonal zirconia crystals embedded in monoclinic zirconia, the strain energy is $\sim 0.46 \times 10^8$ J/m$^2$ [19]. Inserting these values into Eq. (1) gives a critical radius of 6.1 nm. If we assume zero strain energy due to volume expansion of the thin TEM specimen, then $r_c = 4.8$ nm. These values increase with temperature, so in all of these experiments the nanocrystals were well below the critical size for the stabilization of the tetragonal phase.

Based on surface-energy considerations, the formation of tetragonal zirconia nanocrystals is not surprising. What is more surprising is that, considering the extreme radiation resistance of bulk $ZrO_2$, the nanocrystals were amorphized by ion irradiation at a dose of only 0.9 dpa. This is a clear case where size effects and specimen microstructure play a major role in the c–a transition. Based on these observations, a mechanism is required to explain the observed dramatic difference between bulk and nanocrystalline $ZrO_2$.

Phase transitions during irradiation are common in intermetallic alloys and are well understood

from a thermodynamic point of view. According to this picture, point defects, defect complexes, chemical disorder and lattice strain increase the total free energy of a crystal, providing the driving force for a phase transition to higher-energy crystalline or amorphous state [20]. These transitions are similar in many respects to those that occur with increasing temperature [21]. Monoclinic zirconia exhibits precisely this behavior during irradiation. As the free energy of the compound is increased, the tetragonal and subsequently the cubic phase is stabilized. In bulk zirconia, the free energy of the amorphous state is sufficiently high that amorphization does not occur, similar to a number of radiation-resistant intermetallic alloys. From a phenomenological point of view, defects in $ZrO_2$ are sufficiently mobile under irradiation that their concentration saturates well before the onset of amorphization, due to a variety of competing recombination processes [15].

In the nanocrystalline case, the situation is different because the specimen has a higher initial free energy. For $\gamma = 1.10$ J/m$^2$ (corresponding to tetragonal zirconia), and for a radius of 1.5 nm, the free energy of the nanoparticle composite is higher by over 70 kJ/mol prior to the onset of irradiation. This extra surface energy, that is not present in bulk $ZrO_2$, may be sufficient to form the amorphous state. Recent calorimetric experiments concluded that amorphous zirconia is approximately 59.8 kJ/mol less stable than the monoclinic phase [22]. The free energy difference between the tetragonal and monoclinic phase is ~6 kJ/mol at room temperature. Because the extra surface energy (70 kJ/mol) is larger than the apparent free-energy difference between the tetragonal and amorphous structures, one might expect that a spontaneous c–a transformation would occur. However, these calculations ignore the (unknown) surface energy of the amorphous zirconia nanoparticles, which could prevent a spontaneous tetragonal-to-amorphous transformation. Nevertheless, the 70 kJ/mol of surface free energy is considerable, and added to the additional energy provided by particle irradiation, it becomes sufficient to produce the amorphous state.

Other mechanisms may also play a role. For example, ion beam mixing may alter the chemistry of the $ZrO_2$ nanoparticles sufficiently that amorphization might occur. During irradiation, the assemblage of $ZrO_2$ nanoparticles embedded in $SiO_2$ gradually returns to a mixture of amorphous $ZrSiO_4$. Fig. 5(a) shows the original amorphous $ZrSiO_4$ with the mottled contrast typical of an amorphous material. After phase segregation, the $ZrO_2$ nanocrystals are visible as ~3-nm-diameter regions of high contrast (Fig. 5(b)). Fig. 5(c) shows the same specimen after amorphization of the nanoparticles. Clearly, the microstructure is not the same as in Fig. 5(a). In fact, the mottled appearance is still on the order of 3 nm, suggesting that the $ZrO_2$ particles are still present. Furthermore, as discussed earlier, some regions of the specimen were highly depleted in $SiO_2$. Ion beam mixing may play a role in the amorphization of the $ZrO_2$ nanocrystals, but the evidence in Fig. 5 suggests that it is not a major one.

Another possible mechanism is related to the cascade dynamics. In the first few picoseconds after the initial ion impact, a melt-like or plasma-like pocket of interacting, highly energetic atoms is formed. As this region cools to ambient temperature (generally nanoseconds or longer), epitaxial recrystallization occurs adjacent to the still-crystalline material surrounding the cascade.

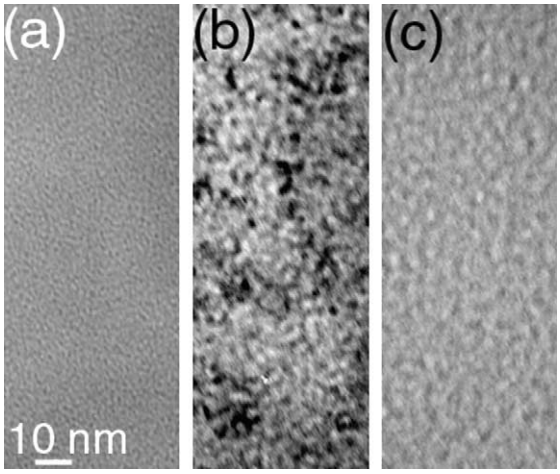


Fig. 5. Bright field images showing (a) amorphous $ZrSiO_4$, (b) thermally precipitated $ZrO_2$ nanocrystals and (c) the specimen in (b) after ion-beam-induced amorphization. All images were taken under identical defocus conditions.

Since a typical cascade size is on the order of 3 nm, in our specimens an entire nanoparticle would be absorbed in a single collision cascade, leaving no surrounding material on which to recrystallize.

We evaluated this hypothesis by performing two experiments: first, we irradiated a $ZrO_2$ nanocomposite with 280 keV $Ne^+$ (i.e. a light ion that produces smaller cascades); and second, we irradiated a gold nanocluster composite with 1.0 MeV Xe ions. The results of the $Ne^+$ irradiation were essentially identical to the 1.0 MeV $Xe^{2+}$ irradiation results. After approximately the same ion dose (the fluence was higher by an order of magnitude), the $ZrO_2$ nanoparticles were amorphized. This suggests that cascade size and shape do not play a major role in the amorphization dynamics, a conclusion that is strengthened by the results of the 1.0 MeV $Xe^+$ irradiation of the Au nanocrystals shown in Fig. 6. The metal nanoparticles showed no indication of amorphization, even at high ion doses. In contrast, the nanoparticles grew slightly larger during irradiation under the same conditions as those in which the $ZrO_2$ nanoparticles became amorphous. If the ion beam mixing or cascade dynamics were important, the Au nanocrystals should also amorphize. From the thermodynamic point of view, however, Au does not have high-temperature metastable phases, it has a relatively low surface free energy, and defects can readily recombine due to lattice site equivalence.

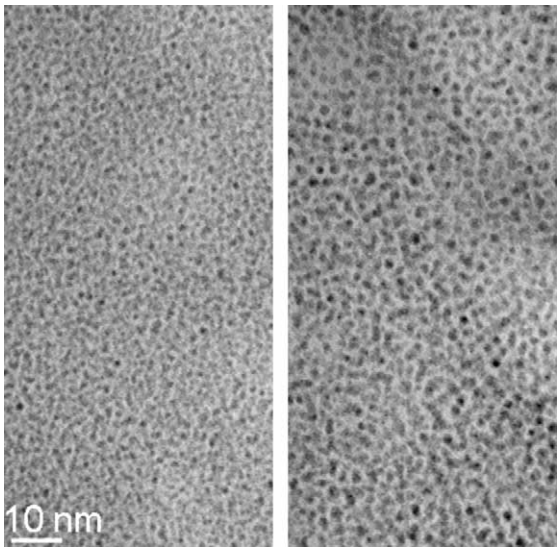


Fig. 6. Au nanoclusters before (left) and after (right) irradiation with 1.0 MeV $Xe^{2+}$. A gold nanocrystal solution was purchased from Nanoprobes, Inc., and the specimen was made by depositing the nanoparticles onto a carbon-coated TEM grid. The as-purchased particles had a nominal diameter of 1.5 nm. After a fluence of approximately $4 \times 10^{14}$ ions/cm$^2$, the average diameter had grown to nearly 3 nm and there was no indication of amorphization.

At higher temperatures, defects in ceramics are more mobile and more rapidly recombine. Therefore, at elevated temperatures the steady-state defect concentration should decrease until, at sufficiently high temperatures, it drops below that required for the crystalline-to-amorphous transition. As shown in Fig. 4, the dose required for amorphization did, in fact, increase slowly at first, but then more rapidly with increasing temperature until, above 450 °C, the zirconia nanoparticles could no longer be amorphized. This type of behavior is consistent with a thermodynamic activation barrier for diffusion-driven defect recombination, as is often reported in ceramic materials.

The present experimental data is most consistent with the defect-driven thermodynamic approach. A considerable body of evidence supports the concept that the irradiation-induced transformation to the amorphous state is in fact a phase transition, and a generalized Lindemann melting criterion has been employed to successfully explain the behavior of intermetallic alloys during irradiation [21]. Some workers have, however, questioned the validity of this concept [23], instead proposing that a percolation-type transition occurs in the case of complex silicates subjected to natural α-decay processes. Each model may be valid in specific cases, since the microscopic mechanism of the c–a transformation can depend strongly on the material properties and irradiation conditions. In the present case, however, the results are consistent with a thermodynamic model in which defect and surface energies add together to produce a higher free-energy state than can be produced in bulk zirconia.

## 5. Conclusions

In this work, we present the first clear and striking example of a *major* shift in the amorphization kinetics of a nanocrystalline ceramic, as compared with its bulk behavior. Bulk $ZrO_2$ has never been amorphized by ion irradiation, regardless of temperature or the mass and energy of the bombarding particles. In direct contrast, we have shown that a composite of embedded tetragonal $ZrO_2$ nanocrystals is readily amorphized, even with ions as light as $Ne^+$. Thermodynamic considerations can be used to explain the formation of tetragonal zirconia. An extension of this thermodynamic argument can also be used to explain the increased susceptibility of nanocrystalline zirconia to amorphization. These results are not, however, universal in the sense that *all* nanophase composites should be susceptible to amorphization, but demonstrate that there can be an important shift in the energetics of amorphization that is no less dramatic than the phase-stability field shifts reported for various nanocrystalline materials. From a technical point of view, for materials used for space applications or other high-radiation applications, knowledge of the radiation resistance of a bulk material may be insufficient to predict the radiation response of nanophase composites.

## Acknowledgements

Irradiations were performed at the IVEM Facility, Argonne National Laboratory. Financial support for this work was provided by NSERC [AM]; USDOE Division of Materials Sciences [LAB]; and Basic Energy Sciences/USDOE Grant #DE-FG02-97ER45656 [RCE].

## References

[1] See R.C. Ewing, Nucl. Instr. and Meth. B 91 (1994) 22.
[2] W.J. Weber, Nucl. Instr. and Meth. 166 (2000) 98.
[3] A.H. Johnston, IEEE Trans Nucl. Sci. 45/3 (1998) 1339.
[4] S.H. Tolbert, A.P. Alivisatos, Science 265 (1994) 373.
[5] G.A. Kachurin, M.O. Ruault, A.K. Gutakovsky, O. Kaitasov, S.G. Yanovskaya, K.S. Zhuravlev, H. Bernas, Nucl. Instr. and Meth. B 147 (1999) 356.
[6] K. Tanabe, T. Yamaguchi, Catal. Today 20 (1994) 185.
[7] E.L. Fleischer, M.G. Norton, M.A. Zaleski, W. Hertl, C.B. Carter, J.W. Mayer, J. Mater. Res. 9 (1991) 1905.
[8] K.E. Sickafus, Hj. Matzke, K. Yasuda, P. Chodak, R.A. Verrall, P.G. Lucuta, H.R. Andrews, A. Turos, R. Fromknecht, N. Baker, Nucl. Instr. and Meth. B 141 (1998) 358.
[9] A. Meldrum, L.A. Boatner, R.C. Ewing, Phys. Rev. Lett. 88 (2002) 025503-1.
[10] H.M. Ondik, H.F. McMurdie (Eds.), Phase Diagrams for Zirconium and Zirconia Systems, American Ceramic Society, Westerville, OH, 1998.
[11] A. Meldrum, S.J. Zinkle, L.A. Boatner, R.C. Ewing, Nature 395 (1998) 56.
[12] J.F. Ziegler, SRIM-2000, IBM Research, Yorktown NY, 1999.
[13] A. Meldrum, L.A. Boatner, S.J. Zinkle, S.X. Wang, L.M. Wang, R.C. Ewing, Can. Mineral. 37 (1999) 207.
[14] W.J. Weber, R.C. Ewing, L.M. Wang, J. Mater. Res. 9 (1994) 688.
[15] K.E. Sickafus, Hj. Matzke, Th. Hartmann, K. Yasuda, J.A. Valdez, P. Chodak, M. Nastasi, R.A. Verrall, J. Nucl. Mater. 274 (1999) 66.
[16] N. Mommer, T. Lee, J.A. Gardner, J. Mater. Res. 15 (2000) 377.
[17] L.M. Wang, S.X. Wang, R.C. Ewing, Philos. Mag. Lett. 80 (2000) 341.
[18] R.C. Garvie, J. Phys. Chem. 82 (1978) 218.
[19] D. Livey, P. Murray, J. Am. Ceram. Soc. 39 (1956) 363.
[20] R.H. de Tendler, C. Rodriguez, L.G. Gallego, J.A. Alonso, J. Mater. Sci. 31 (1996) 6395.
[21] N.Q. Lam, P.R. Okamoto, M. Li, J. Nucl. Mater. 251 (1997) 89.
[22] I. Molodetsky, A. Navrotsky, M.J. Paskowitz, V.J. Leppert, S. Risbud, J. Non-Cryst. Sol. 262 (2000) 106.
[23] E.K.H. Salje, J. Chrosch, R.C. Ewing, Am. Mineral. 84 (1999) 1107.